



Mixture effects of oxygenated PAHs and benzo[a]pyrene on cardiovascular development and function in zebrafish embryos

Virgínia Cunha^{a,1}, Carolina Vogts^{b,c,1}, Florane Le Bihanic^{a,2}, Kristian Dreij^{a,*}

^a Unit of Biochemical Toxicology, Institute of Environmental Medicine, Karolinska Institutet, Box 210, 171 77 Stockholm, Sweden

^b Unit of Integrative Toxicology, Institute of Environmental Medicine, Karolinska Institutet, Box 210, 171 77 Stockholm, Sweden

^c Pharmacology and Toxicology Unit, Department of Biomedical Science and Veterinary Public Health, Swedish University of Agricultural Sciences, Box 7028, 750 07 Uppsala, Sweden

ARTICLE INFO

Handling Editor: Frederic Coulon

Keywords:

Oxy-PAHs

Benzo[a]pyrene

Mixture effects

Zebrafish

Cardiovascular toxicity

Ah receptor-dependent

ABSTRACT

Polycyclic aromatic compounds (PACs), including polycyclic aromatic hydrocarbons (PAHs) and oxygenated PAHs (oxy-PAHs), are common environmental pollutants known to cause health effects in humans and wild-life. In particular, vertebrate cardiovascular development and function are sensitive to PACs. However, the interactive effects of PAHs and oxy-PAHs on cardiovascular endpoints have not been well studied. In this study, we used zebrafish embryos (ZFEs) as a model to examine developmental and cardiovascular toxicities induced by the three environmental oxy-PAHs benzo[a]fluorenone (BFLO), 4H-cyclopenta[def]phenanthren-4-one (4H-CPO) and, 6H-benzo[cd]pyren-6-one (6H-BPO), and the PAH benzo[a]pyrene (BaP) either as single exposures or binary oxy-PAH + PAH mixtures. 6H-BPO induced developmental and cardiovascular toxicity, including reduced heartbeat rate and blood flow, at lower doses compared to the other compounds. Exposure to binary mixtures generally caused enhanced toxicity and induction of aryl hydrocarbon receptor (AhR)-regulated gene expression (*ahr2* and *cyp1a*) compared to single compound exposure. This was associated with differential expression of genes involved in cardiovascular development and function including *atp2a2*, *myh6*, *tbx5* and *zerg*. AhR-knock-down significantly reduced the cardiovascular toxicity of 6H-BPO and its binary mixture with BaP indicating a significant AhR-dependence of the effects. Measurements of internal concentrations showed that the toxicokinetics of BaP and 6H-BPO were altered in the binary mixture compared to the single compound exposure, and most likely due to CYP1 inhibition by 6H-BPO. Altogether, these data support that similar to interactions between PAHs, mixtures of PAHs and oxy-PAHs may cause increased developmental and cardiovascular toxicity in ZFEs through an AhR-dependent mechanism.

1. Introduction

Polycyclic aromatic hydrocarbons (PAHs) are ubiquitous environmental toxic contaminants and have been established to cause genotoxicity, developmental and cardiac toxicity in exposed organisms (Billiard et al., 2008; IARC, 2010; Geier et al., 2018). The regulation of PAHs has been restricted to benzo[a]pyrene (BaP) and 27 other priority PAHs as designated by the U.S. Environmental Protection Agency (U.S. EPA) and European Union (EU) (European Union, 2005; U.S. EPA, 2010). However, chemicals are present in the environment in intricate mixtures and PAHs are no exception. Other classes of polycyclic aromatic compounds (PACs) such as oxygenated PAHs (oxy-PAHs) are normally found together with PAHs in the environment and can thus

contribute to the toxicity significantly (Lundstedt et al., 2007).

Oxy-PAHs are widely spread in the environment and can be found in similar or higher levels than their parent compounds (Lundstedt et al., 2007). In addition, they are more mobile in the environment, which can result in higher bioavailability and elevated risk for human health and the environment (Lundstedt et al., 2007; Layshock et al., 2010; Idowu et al., 2019). Bandowe et al. showed that measured concentrations of Σ15 oxy-PAHs in various fish species were higher than Σ16 US EPA priority PAHs (Bandowe et al., 2014). Although PAHs, oxy-PAHs and other PACs are normally present in mixtures, few studies have focused on the effects of these mixtures. Using environmental PAC samples obtained from contaminated soils, Wincent et al showed that the polar fraction including oxy-PAHs may cause enhanced or similar

* Corresponding author.

E-mail address: Kristian.Dreij@ki.se (K. Dreij).

¹ Shared authorship.

² Present address: Laboratoire EPOC, UMR CNRS 5805, Université de Bordeaux, 33405 Talence Cedex, France.

developmental toxicity in fish compared to the non-polar PAH fraction (Wincent et al., 2015a). Exposures to single oxy-PAHs show developmental and genotoxic effects in zebrafish (*Danio rerio*) and Japanese medaka (*Oryzias latipes*) (Knecht et al., 2013; Dasgupta et al., 2014; Geier et al., 2018; McCarrick et al., 2019). It is further unknown whether toxicokinetic processes are altered in a mixture exposure compared to single exposure. Therefore, more studies are needed to understand the interactions between PAHs and other PACs on toxicokinetic and toxicodynamic processes.

Cardiac development is particularly sensitive to environmental pollution (Sarmah and Marrs, 2016) and cardiotoxicity due to PAH exposure is well established. Different experimental and epidemiological studies indicate the involvement of PAHs in the pathogenesis of cardiovascular diseases in humans (Korashy and El-Kadi, 2006; Holme et al., 2019). Persistent cardiac damage has also been observed in fish exposed to oil spills or sediments at PAH contaminated sites (Incardona et al., 2014, 2015; Brown et al., 2017). Due to the conserved physiology compared to humans, zebrafish (*D. rerio*) has increasingly been used as a model for studying cardiotoxicity, cardiac development and cardiac disease (MacRae and Peterson, 2015; Sarmah and Marrs, 2016). Cardiac development in zebrafish can be observed throughout embryogenesis and is divided in two phases. In the first phase, which takes place from 0 to 28 h post fertilization (hpf), the primitive tube heart develops. In the second phase, the separation of late-differentiating cardiomyocytes form two chambers and looping of the heart occurs, resulting in a two chambered heart at around 48 hpf (de Pater et al., 2009; Miura and Deborah, 2011). Cardiac defects, caused by xenobiotics for example, may manifest by pericardial edema or deficient looping of the heart resulting in tubular or so-called string heart that may cause disruption of heart rhythm (e.g. arrhythmia and bradycardia) and reduced blood flow (Miura and Deborah, 2011; Incardona et al., 2014; Le Bihanic et al., 2015). Importantly, cardiotoxicity has been shown to be an early event in PAC toxicity in fish, with morphological deformities as secondary effects (Incardona et al., 2004).

To date, the mechanism of PAC-induced cardiotoxicity in fish has not been fully understood. Available data show that PAHs can induce cardiotoxicity through activation of the aryl hydrocarbon receptor (AhR) and subsequent *CYP1A* induction, leading to morphological and functional defects on the cardiovascular system in zebrafish (Incardona et al., 2011; Van Tiem and Di Giulio, 2011). In contrast, PAH mixtures derived from crude oil or smaller tricyclic PAHs, such as phenanthrene, cause cardiotoxicity in an AhR-independent manner, leading to cardiac function impairment and morphological deformities (Incardona et al., 2004, 2005; Brette et al., 2017). Deregulation of AhR activation and signaling has also been suggested to be involved in the observed non-additive genotoxic and tumorigenic effects of simple and complex PAH mixtures (Jarvis et al., 2014). Recent studies have demonstrated that PAHs can cause cardiotoxicity by impairing the excitation–contraction (EC) coupling in fish heart (Brette et al., 2014, 2017a). Although previous studies have indicated both AhR-dependent and -independent mechanisms in zebrafish, relatively little is known about how oxy-PAHs and other polar PACs cause cardiotoxicity (Knecht et al., 2013; Goodale et al., 2015; Geier et al., 2018). We have previously shown that the oxy-PAHs benzo[*a*]fluorenone (BFLO) and 6*H*-benzo[*cd*]pyren-6-one (6H-BPO) efficiently inhibited AhR activation by 2,3,7,8-tetrachlorodibenzo-*p*-dioxin (TCDD) in human HaCaT cells (Wincent et al., 2016), suggesting that interaction effects might arise from PAC mixtures.

This work aimed to determine the effects of binary PAH/oxy-PAH mixtures on the developing zebrafish embryo with focus on the cardiotoxicity of these compounds. To this end, developmental and cardiovascular toxicities were assessed in zebrafish embryos exposed to single oxy-PAHs or in combination with BaP. Moreover, expression levels of genes and proteins related with AhR-signaling and cardiovascular development and function were measured. The role of AhR-signaling was investigated by use of morpholinos targeting the zebrafish AhR gene

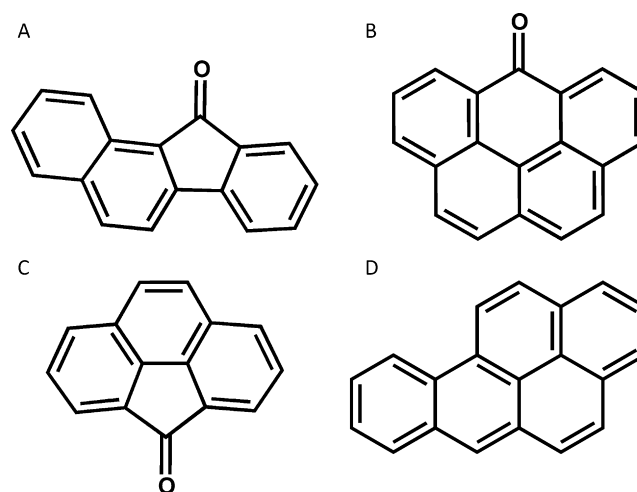


Fig. 1. Chemical structures of PACs used in the study; benzo[*a*]fluorenone (A, BFLO), 6*H*-benzo[*cd*]pyren-6-one (B, 6H-BPO), 4*H*-cyclopenta[*def*]phenanthrene-4-one (C, 4H-CPO), and benzo[*a*]pyrene (D, BaP).

ahr2. In addition, we measured internal concentrations of these compounds alone and in a mixture to better understand the toxicokinetic processes including possible toxicokinetic and toxicodynamic alterations.

2. Material and methods

2.1. Chemicals

The three ketone oxy-PAHs benzo[*a*]fluorenone (BFLO) (CAS-Nr 479-79-8), 4*H*-cyclopenta[*def*]phenanthren-4-one (4H-CPO) (CAS-Nr 5737-13-3) and 6*H*-benzo[*cd*]pyren-6-one (6H-BPO) (CAS-Nr 3074-00-8), all with purity $\geq 99\%$, were obtained from the Institute for Reference Materials and Measurements (EC-JRC-IRMM, Belgium). Chemical structures are shown in Fig. 1. Benzo[*a*]pyrene (BaP) (CAS-Nr 50-32-8; purity $\geq 96\%$), dimethyl sulfoxide (DMSO, purity 96%) and pyrene (CAS-Nr 129-00-0; purity 99%) were obtained from Sigma Aldrich, Sweden. Acetonitrile (ACN, gradient grade for HPLC) was obtained from VWR, Sweden.

2.2. Zebrafish and exposure

Zebrafish embryos (ZFEs) of AB wild-type strain and transgenic cardiac myosin light chain 2 [Tg (*cm1c2:GFP*)] were used in the experiments. Fertilized eggs were obtained from the Zebrafish Core Facility at Comparative Medicine, Karolinska Institutet, and held at 28 °C in embryo medium (EM, 5.0 mM NaCl, 0.17 mM KCl, 0.33 mM CaCl₂, 0.33 mM MgSO₄) in a thermo-regulated chamber (IPP110 plus, Memmert, Germany). At 24 h post fertilization (hpf), groups of 30 embryos (in 30 mL) per replicate were exposed to 0.1–1 μ M single compound, a mixture of oxy-PAH plus BaP (1 μ M), or solvent control (0.01% DMSO (v/v)) up to 120 hpf. Due to solubility issues, 6H-BPO was used up to 0.5 μ M. Compounds dissolved in DMSO were added directly to EM and immediately mixed by gently swirling the dish. All exposures were performed in glass Petri dishes and all given concentrations are nominal concentrations unless otherwise stated. All experiments were performed in at least triplicates.

2.3. AhR knock-down in zebrafish by morpholinos

Knock-down of AhR was performed as previously described (Wincent et al., 2015a). A morpholino antisense oligonucleotide targeting *ahr2* (*ahr2*-MO; 5'-TGTTACCGATACCCGCCGACATGGTT- 3') and blocking its translation (Prasch et al., 2003) and a negative control

morpholino (CT-MO; 5'-CCTCTTACCTCAGTTACAATTATA-3') (Gene Tools, Philomath, OR) were used. Both morpholinos (0.15 mM) were injected into Tg (*cmIc2:GFP*) embryos at 2- to 4-cell stage using an Eppendorf FemtoJet injector (Eppendorf, Germany). At 6–8 hpf, ZFEs were screened by fluorescence microscopy to verify incorporation of morpholinos. Damaged embryos or those not displaying homogeneous fluorescence were removed.

2.4. Determination of toxicokinetics

Three different exposure scenarios were set-up for determining the toxicokinetics of either 6H-BPO and BaP alone or as a mixture in ZFEs according to Vogs et al. (2019). First, a “ZFE-free medium” consisting of EM without ZFE was prepared to rule out unspecific loss due to chemical adsorption to glass surface, hydrolysis or evaporation. Second, a “biological control” was set up by incubating ZFE in EM without addition of chemical. Third, ZFEs were exposed as described above with one ZFE per mL EM. Exposures took place from 24 hpf up to 120 hpf and samples were collected at 27, 30, 33, 48, 55, 72, 96 and 120 hpf. Triplicates of 300 μ L aliquots from EM samples of both ZFE-free control and ZFE-medium were transferred to amber HPLC glass vials (2 mL, Agilent, Sweden). Five replicates per sample time point consisting of five ZFEs were collected in 1.5 mL Eppendorf microtubes, excessive EM was discarded and ZFE were washed with double-distilled water (ddH_2O) two times. All samples were stored at -80 °C until further sample preparation and chemical analysis.

Before analysis by high performance liquid chromatography (HPLC), 700 μ L of an internal standard (10 μ M pyrene dissolved in 100% ACN) was added to EM samples. To the ZFE samples, 300 μ L of the internal standard dissolved in ACN: ddH_2O (70%:30%, v:v) was added followed by homogenization using 1 mm diameter zirconium oxide beads (Next Advance, NY). The supernatant was transferred to clean 1.5 mL tubes. Remaining beads were washed once with 100 μ L of ACN: ddH_2O (70%:30%, v:v) and the supernatant subsequently added to the ZFE homogenate in order to account for chemical adsorption at the beads' surface. The homogenate was cleared by centrifugation at 14 000 rpm for 5 min and the final supernatant transferred to amber HPLC glass vials.

EM and ZFE samples were analyzed using an YL9100 HPLC system equipped with an Agilent 1100 UV detector (both from Dalco ChromTech, Sweden). PACs were separated on a 150 mm long, 5 μ m particle size reverse phase ACE C18-AR column (Scantec Lab, Sweden) using a 25 min gradient elution. Gradient was from 70% B to 100% B for 22 min and then back to 70% B at 25 min (solvent A, 1.5 mM formic acid in ddH_2O ; solvent B, 1.5 mM formic acid in ACN) at a flow rate of 1 mL/min. 6H-BPO and BaP were detected by UV at 250 nm and 254 nm, respectively, and quantified according to respective calibration curves. Outliers were identified by nonlinear regressions using the ROUT method in GraphPad Prism 7 and removed.

The concentration declines in the ZFE-free medium and ZFE medium (C_w in μ M L^{-1}) were simulated using an exponential function with the decay rate constant k_w [h^{-1}]:

$$\frac{dC_w(t)}{dt} = -k_w \times C_w$$

A one-compartment model was used to simulate the time courses of the internal concentrations (C_{int} in μ M L^{-1} ZFE volume (= μ M)):

$$\frac{dC_{int}(t)}{dt} = k_{in} \times C_w - (k_{out} + k_m) \times C_{int}$$

where k_{in} is the uptake rate constant (h^{-1}), k_{out} the elimination rate constant (h^{-1}) and k_m the biotransformation rate constant (h^{-1}). In addition, the biotransformation capacity k_m was assumed to linearly increase over time to obtain better fitting results. All simulations were conducted in Berkeley Madonna (version 8.3.18).

2.5. Assessment of morphological effects and mortality

At 96 hpf, ZFEs were assessed under a Nikon SMZ25 microscope (Nikon, Japan) and selected endpoints (mortality, pericardial and yolk sac edema, swim-bladder inflation, string heart) were scored (%) as being either present or absent. Zebrafish mortality was controlled every day during exposure time and dead embryos were discarded daily. Cumulative effects were calculated at 96 hpf as the sum of lethal or sublethal endpoints. Results are expressed as mean \pm SE of 3–10 replicates with a pool of 10 embryos per replicate.

2.6. Cardiac function analysis

For cardiac function analysis, heartbeat rate and blood flow at the caudal vein were recorded on 26–86 individual ZFEs per condition at 96 hpf using a Nikon SMZ25 microscope and NIS-Elements Imaging Software (Nikon, Japan). Prior to analysis, ZFEs (5 per well in a 24-well plate) were anesthetized (0.168 mg/mL tricaine solution, Sigma Aldrich, Sweden) for 1–3 min. Next, the ZFEs were placed in a drop of 3% methylcellulose in a petri-dish and incubated for 3 min in dark at 28 °C. The petri-dish was placed under the microscope equipped with a glass heating plate set at 28 °C (Okolab, Italy), and left to acclimatize for 2 min. The recording of the video was made with a frame rate at around 17 fps and 2560 \times 1920 resolution and for 10 sec. Effects on cardiac function were assessed by measuring heartbeat rate and blood flow using the DanioScope software (Noldus, Netherlands) according to instructions. The heart area was determined by manually tracing the heart with DanioScope software tools. To measure blood flow, videos containing up to 5 larvae were recorded using a microscope magnification at 20x. In DanioScope, the area of the blood vessel was selected using a circle with a diameter of 2 mm \pm 0.5 mm. The area was copied to all larvae present in the same video to ensure standardization. In both cases, DanioScope uses changes in pixels on a frame-by-frame basis to measure the endpoints. The heart rate is reported as number of beats per minute (BPM) and the blood flow in a percentage of activity within that area (%) by DanioScope.

2.7. In vivo EROD activity measurement

Ethoxyresorufin-O-deethylase (EROD) activity *in vivo* was measured according to previous published protocol (Perrichon et al., 2014) with some minor changes. At 96 hpf, a total number of 10 larvae per treatment were selected and divided into two wells in a 24-well plate (five individuals per well). The exposure solution was replaced by 1 μ M 7-ethoxyresorufin (Sigma Aldrich, Sweden) in EM. After 3 h incubation in dark, the fluorescence of the incubation media was measured in duplicate. Production of resorufin was determined using a Victor 3 Wallac plate reader (Perkin Elmer, MA) with ex/em: 560/590 nm and results were expressed as pmol of resorufin produced/larvae/min. A standard curve of EROD activity was performed using resorufin dilutions.

2.8. RNA purification and quantitative Real-Time PCR (qRT-PCR)

Samples of group replicates composed of 10 pooled larvae were collected at 96 hpf for gene expression analysis and stored in RNAlater (Sigma Aldrich, Sweden). RNA from zebrafish was purified using ReliaPrep RNA Tissue Miniprep System kit (Promega, Sweden) followed by cDNA synthesis using High-Capacity cDNA Reverse Transcription kit (Applied Biosystems, Sweden) according to manufacturer's protocols. RNA quantification and quality were verified by measurement of the ratio of optical density at λ 260/280 nm using NanoDrop 1000 (Thermo Scientific, Sweden). Reactions for qRT-PCR were performed on an Applied Biosystem 7500 Real-Time PCR system (Applied Biosystem, Foster City, CA) using Maxima SYBR Green qPCR Master Mix (Thermo Fisher, Sweden). Conditions were as follows: 95 °C for 2 min, and then 40 cycles at 95 °C for 15 s and 60 °C for 1 min. At the end of each run, a

melting curve analysis was done to determine the formation of the specific products. The relative expression ratio was calculated with comparative threshold cycle method ($2^{-\Delta\Delta Ct}$) using *l13* as reference gene. Primer sequences are given in Table S1.

2.9. Western blot

At 96 hpf, 30 larvae were transferred to pre-chilled tubes with EM and the yolk was mechanically disrupted. Each sample was homogenized in $1 \times$ IPB7 lysis buffer supplemented with Halt™ Protease and Phosphatase Single-use Inhibitor Cocktail (Thermo Scientific, Sweden) and PMSF (Sigma-Aldrich, Sweden) and snap frozen in cryotubes using liquid N_2 . Protein concentrations were measured by Bradford method (Bradford, 1976), and samples were further processed and analyzed by immunoblotting as previously described (Edmunds et al., 2015). The proteins were detected using antibodies against Tbx5 (1:1000, cat no. ARP33403) and Zerg (1:500, cat no. P35480) from Aviva Systems Biology, San Diego, CA. Actin was used as loading control (1:1000, cat no. sc-1615, Santa Cruz Biotechnology, Santa Cruz, CA). Proteins were visualized with enhanced chemiluminescence (Amersham Biosciences, Sweden). Densitometry analysis was performed using ImageJ software (National Institute of Health, USA). The experiments were performed at least in triplicates.

2.10. Statistics

Data are presented as mean \pm standard error. Analysis of variance among exposures compared to control was evaluated by Kruskal-Wallis or one-way ANOVA, followed by a multiple comparison test (Dunn's test and Bonferroni's test, respectively). For binary mixtures with a significant effect on morphological and functional endpoints, this was followed up by a statistical analysis in comparison with oxy-PAH alone using a two-sided Student's *t*-test. Data from mRNA expression were log transformed to fit ANOVA assumptions. Statistical significance of deviation from additive effects on gene and protein expression were determined using a two-sided Student's *t*-test with a False Discovery Rate approach ($Q = 10\%$) to adjust for multiple testing. For this analysis, additive effects were estimated by summing the values from the single exposures (BaP plus BFLO, 4H-CPO or 6H-BPO, respectively) and subsequently compared to the observed effects from the binary oxy-PAH + BaP exposure. Tests were performed using Statistica 7 (Statsoft, Inc) or GraphPad Prism 7 (GraphPad Software, Inc). Principal component analysis (PCA, two axes) of the exposures and the different measured endpoints was performed using R software coupled with the FactoMineR package (Le et al., 2008). Correlation analyses between morphological and functional endpoints were based on Pearson's correlation coefficients with two-tailed *p*-values. The criterion for significance was set at $P < 0.05$.

3. Results

3.1. Effects on morphological and cardiovascular endpoints

Developmental toxicity including mortality following exposure to different concentrations of BFLO, 4H-CPO, 6H-BPO, BaP or PAH + oxy-PAH combinations at 96 hpf are presented in Table 1. Mortality was not increased in response to any exposure. Exposure to BaP alone at $1 \mu M$ did not induce any significant effects on either morphological or functional endpoints, although about one third of the ZFEs did not have inflated swim-bladder at 96 hpf ($P = 0.07$). Results further showed that 6H-BPO was the most potent developmental toxicant with decreased swim-bladder inflation starting from the lowest dose of $0.1 \mu M$ ($P < 0.01$) and an increased incidence of pericardial edema from $0.3 \mu M$ ($P < 0.05$). Moreover, 6H-BPO was the only oxy-PAH that induced string heart formation. All oxy-PAHs caused a reduced heart-beat rate, up to a 20% reduction in the case of 6H-BPO ($P < 0.001$),

although a clear dose-response could not be observed. In agreement with the formation of string heart and reduced heartbeat rate, 6H-BPO reduced the blood flow in the caudal vein more than 8-fold compared to control (0.6 vs 5.0% , $P < 0.0001$). Notably, a large proportion of these embryos completely lacked circulating red blood cells. The other two oxy-PAHs did not reduce the blood flow when applied as single compounds. A combined exposure of BFLO or 4H-CPO with BaP did not increase the incidence of morphological effects compared to single compound exposures. However, both heartbeat rate and blood flow were more strongly reduced by these binary mixtures compared to control ($P < 0.05 - 0.0001$) and in the case of BFLO + BaP also compared to the oxy-PAH alone ($P < 0.05$). Exposure to the combination of 6H-BPO and BaP increased the incidence of both yolk sac and pericardial edema, both in comparison with control and oxy-PAH alone ($P < 0.05 - 0.001$). Notably, the blood flow was increased in response to the binary exposure compared to oxy-PAH alone (3.1 vs 0.6% , $P < 0.05$), but still decreased compared to control ($P < 0.01$). In summary, among the three tested oxy-PAHs 6H-BPO was the most potent developmental and cardiovascular toxicant and the effects were further increased when co-exposed with BaP.

3.2. Effects on AhR signaling and CYP1 activity

In previous *in vitro* and *in vivo* studies, oxy-PAHs have been shown to both activate and inhibit AhR signaling and cytochrome P450 family member 1 (CYP1) activity (Knecht et al., 2013; Wincent et al., 2016). To comprehend the impact of BFLO, 4H-CPO, and 6H-BPO alone and in combination with BaP in ZFEs, gene expression levels of cytochrome P450 family member 1a (*cyp1a*) and AhR (*ahr2*), as well as CYP1 enzyme activity (EROD activity) were investigated. In embryos exposed to oxy-PAHs alone, mRNA expression of *cyp1a* and *ahr2* was decreased for most of the concentrations compared to control (Fig. 2A and B). This down regulation was enhanced for *ahr2* ($0.02 - 0.07$ -fold, $P < 0.05 - 0.0001$). Exposure to $1 \mu M$ BaP resulted in induced expression of *cyp1a* (4-fold, $P < 0.05$) and reduced expression of *ahr2* (0.06 -fold, $P < 0.001$) compared to control. In general, an upregulation in gene expression was observed in embryos exposed to the binary mixtures. The combined exposure of $0.3 \mu M$ 4H-CPO or 6H-BPO with BaP resulted in a more than additive increased *cyp1a* expression (6.5 - and 14.9 -fold, $P < 0.05 - 0.01$) compared to single compound exposure. In contrast, the mixture of BFLO and BaP caused a more than additive decreased *cyp1a* expression at all doses ($P < 0.001$). For *ahr2*, the effect of the binary mixtures with BFLO and 4H-CPO was the reverse compared to single compound exposures, resulting in an up to 4-fold increase of expression. This was especially evident for the mixtures with 0.1 and $1 \mu M$ BFLO and $0.3 \mu M$ 4H-CPO ($P < 0.05 - 0.01$). The mixture of 6H-BPO + BaP did not result in any interaction effects and resulted in similarly reduced *ahr2* expression levels as for single compound exposures. Measurements of CYP1 enzyme activity did not reveal any clear effects (Fig. 2C). Single compound exposures did not result in changes in EROD activity. A trend was observed that the binary mixtures increased enzyme activity, which was especially clear for BFLO + BaP ($P < 0.05$), compared to control. In total, these results indicate a complex pattern of interaction effects of oxy-PAHs and BaP on AhR signaling, which might be related to the observed morphological and functional effects.

3.3. Effects on regulators of cardiac development and function

To understand the interaction effects of oxy-PAHs and PAHs on the cardiac development and function in ZFEs, we evaluated expression of mRNA transcripts of a set of genes encoding proteins that play a key role in these functions (Fig. 3). The four selected genes can be divided in two groups according to their related function. (i) Genes associated with excitation-contraction (EC) coupling; the calcium transport ATPase encoded by *atp2a2* and the potassium voltage-gated channel

Table 1
Effects on morphological endpoints, heartbeat and blood flow at 96 hpf after exposure to oxy-PAHs alone or in combination with BaP (1 μ M).

Condition	Concentration (μ M)	Mortality (%)	Swim-bladder inflation (%)	Yolk-sac edema (%)	Pericardial edema (%)	String heart (%)	Heartbeat (BPM)	Rel. heartbeat	Blood flow (%)	Rel. blood flow
Solvent control	0	1.0 \pm 1.0 ^a	94 \pm 2.2	0	0	0	187 \pm 5		5.1 \pm 0.4	
BFLO	0.1	0	83 \pm 8.8	0	3.3 \pm 3.3	0	167 \pm 4	↓	nd ^b	
	0.3	3.3 \pm 3.3	77 \pm 6.7	0	0	0	172 \pm 6	↓	4.1 \pm 0.4	≈
	1	3.3 \pm 3.3	77 \pm 3.3	0	3.3 \pm 3.3	0	183 \pm 4	≈	nd	
BFLO + BaP	0.1	3.3 \pm 3.3	77 \pm 6.7	0	3.3 \pm 3.3	3.3 \pm 3.3	153 \pm 4 ^{****, ‡}	↓↓↓	nd	
	0.3	0	73 \pm 22	0	10 \pm 0	6.7 \pm 6.7	182 \pm 5	≈	2.3 \pm 0.3 ^{****, ‡}	↓↓
	1	6.7 \pm 3.3	63 \pm 8.8	0	6.7 \pm 6.7	0	169 \pm 5	↓	nd	
4H-CPO	0.1	0	83 \pm 8.8	0	0	0	169 \pm 4	↓	nd	
	0.3	6.7 \pm 6.7	93 \pm 3.3	0	3.3 \pm 3.3	0	168 \pm 6	↓	4.2 \pm 0.4	≈
	1	3.3 \pm 3.3	73 \pm 6.7	0	3.3 \pm 3.3	0	164 \pm 7 [*]	↓↓	nd	
4H-CPO + BaP	0.1	3.3 \pm 3.3	70 \pm 10	0	3.3 \pm 3.3	0	190 \pm 4	≈	nd	
	0.3	6.7 \pm 6.7	83 \pm 3.3	0	3.3 \pm 3.3	0	174 \pm 6	↓	3.5 \pm 0.4 [*]	↓
	1	3.3 \pm 3.3	83 \pm 3.3	0	0	0	144 \pm 7 ^{***}	↓↓↓	nd	
6H-BPO	0.1	3.3 \pm 3.3	37 \pm 6.7 ^{**}	0	27 \pm 15	0	178 \pm 3	↓	nd	
	0.3	6.7 \pm 3.3	23 \pm 8.8 ^{***}	0	53 \pm 22 [*]	13 \pm 8.8	154 \pm 6 ^{***}	↓↓↓	0.6 \pm 0.2 ^{****}	↓↓↓
	0.5	3.3 \pm 3.3	43 \pm 17 [*]	3.3 \pm 3.3	33 \pm 23	13 \pm 3.3 [*]	161 \pm 8 ^{**}	↓↓	nd	
6H-BPO + BaP	0.1	0	53 \pm 13	0	20 \pm 5.8	13 \pm 13	180 \pm 5	≈	nd	
	0.3	10 \pm 10	40 \pm 12 ^{**}	6.7 \pm 3.3 ^{**}	47 \pm 19 [*]	47 \pm 6.7 ^{***}	162 \pm 6 [*]	↓↓	3.1 \pm 0.4 ^{**‡}	↓
	0.5	6.7 \pm 6.7	33 \pm 17 ^{**}	3.3 \pm 3.3	67 \pm 18 ^{**}	57 \pm 26 ^{**}	165 \pm 6 [*]	↓↓	nd	
BaP	1	1.4 \pm 1.4	67 \pm 6.0	2.9 \pm 1.8	7.1 \pm 4.2	1.4 \pm 1.4	192 \pm 5	≈	3.8 \pm 0.4	≈

^a Results are presented as mean \pm standard error, $n = 3 - 10$ replicates for morphological endpoints and $n = 26 - 86$ ZFEs for heartbeat and blood flow.

^b nd = not determined.

* $P < 0.05$.

** $P < 0.01$.

*** $P < 0.001$.

**** $P < 0.0001$ as compared to control by Kruskal-Wallis (morphological endpoints) or one-way ANOVA (functional endpoints).

‡ $P > 0.05$ as compared to oxy-PAH alone by Student's t -test.

encoded by *zerg* (also known as *kcnh2*). (ii) Genes associated with cardiac development and function; myosin heavy chain encoded by *myh6*, the T-box transcription factor encoded by *tbx5*, and troponin T encoded by *tnnt2*.

The results showed that mixtures of oxy-PAHs and PAHs could disrupt mRNA expression of genes coding for proteins involved in EC coupling (Fig. 3A and B). Expression of *atp2a2* was upregulated by exposure to BaP (3.9-fold, $P < 0.05$) and showed a tendency to be upregulated by BFLO and 4H-CPO (> 2 -fold but $P > 0.05$). *Atp2a2* was the only gene whose expression was affected by BaP. For all oxy-PAHs, exposure to the binary mixture with BaP caused a more than additive repression of induction of *atp2a2* compared to the single compounds at one or more doses ($P < 0.05 - 0.01$). For *zerg*, exposure to BaP, BFLO or 4H-CPO did not affect gene expression levels while 6H-BPO increased expression levels at the two higher doses about 5-fold but with $P > 0.05$. A trend could be observed that the binary mixtures further induced *zerg* expression levels, which was especially evident for 0.1 μ M 4H-CPO + BAP compared to single compounds ($P < 0.05$). For genes involved in cardiac development (Fig. 3C - E), the results showed that expression levels of *myh6* were induced about 6-fold by 0.5 μ M 6H-BPO ($P < 0.05$) compared to control, which became repressed when co-exposed to BaP (0.45-fold, $P < 0.05$). Similar to *ahr2*, the binary mixture of 4H-CPO + BaP caused the reverse effect of the individual compounds, with up to 5.4-fold induction of *myh6* by the mixture with 0.3 μ M 4H-CPO ($P < 0.01$ compared to control and $P < 0.0001$ compared to the single compounds). For *tbx5*, strongest effects were observed in response to 6H-BPO, both alone and in combination with BaP, with an up to 12-fold induction of expression ($P < 0.05$) compared to control. Similar to *myh6*, the binary mixture of 4H-CPO and BaP caused a more than additive induction of *tbx5* expression compared to single compounds ($P < 0.01$). Expression levels of *tnnt2* were in general unaffected, although a tendency of repressed expression levels

in response to BFLO and 4H-CPO were observed (> 0.5 -fold but $P > 0.05$). Altogether, the results indicate that binary mixtures showed a more than additive effect on the selected genes related in cardiac development and function compared to single PACs exposure.

The protein levels of Tbx5 and Zerg in the ZFE were evaluated (Fig. 4A and B). Both protein levels were increased in embryos exposed to oxy-PAHs alone and in combination with BaP, especially Zerg in response to 4H-CPO and 6H-BPO alone ($P < 0.05 - 0.01$), and 6H-BPO + BaP. These data support the gene expression results, especially for 6H-BPO and Zerg.

3.4. Role of AhR activation and impact on toxicokinetics

Based on its high potency, the mixture of 6H-BPO and BaP was chosen for further studies with the aim to investigate the role of AhR and if the mixture exposure affected their toxicokinetics. Knock-down of AhR with morpholinos against *ahr2* (MO_AhR) in ZFEs clearly rescued the cardiotoxic effects caused by BaP (1 μ M), 6H-BPO (0.3 μ M) and their binary mixture (Fig. 5 and Table 2). For example, the high incidence of pericardial edema (60%) and string heart formation (43%) in response to the binary mixture was completely abolished. Similarly, knock-down of AhR rescued the heartbeat rate and blood flow to levels similar to control ZFE ($P < 0.01 - 0.0001$).

We further investigated the toxicokinetics of 6H-BPO and BaP alone and in combination (Fig. 6, Table S2). Initial concentrations of 6H-BPO and BaP were 0.61 μ M and 0.67 μ M; 50% higher and 30% lower than the nominal exposures used for the effect characterizations (0.3 and 1 μ M, respectively). Concentrations decreased in ZFE-free medium and in ZFE medium for both single exposure and mixture exposure (Fig. 6A, B, C, D). The decline of BaP in the ZFE-free medium and ZFE medium was similar, while 6H-BPO decreased twice as fast in the ZFE medium than in the ZFE-free medium. These results indicated that both

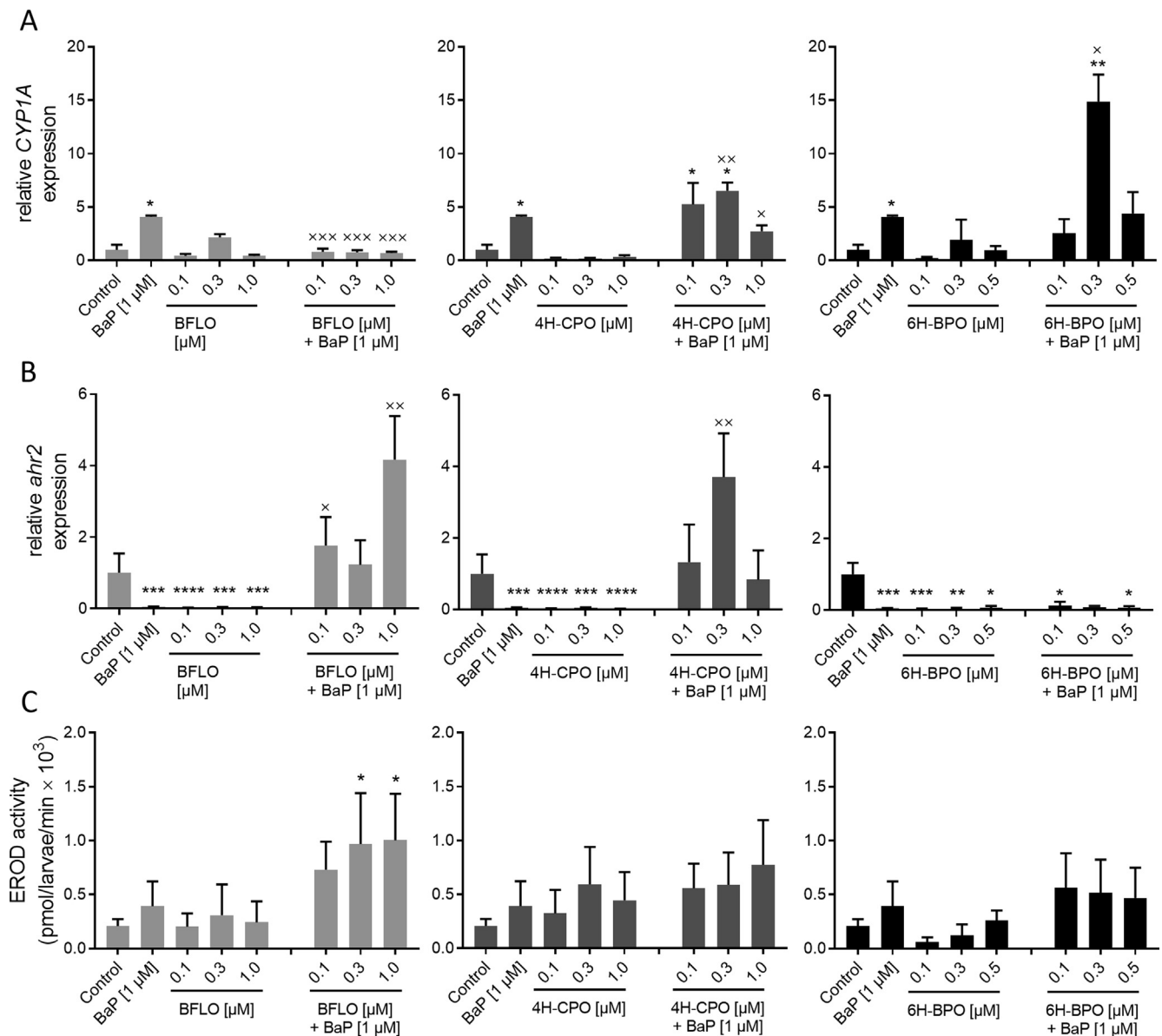


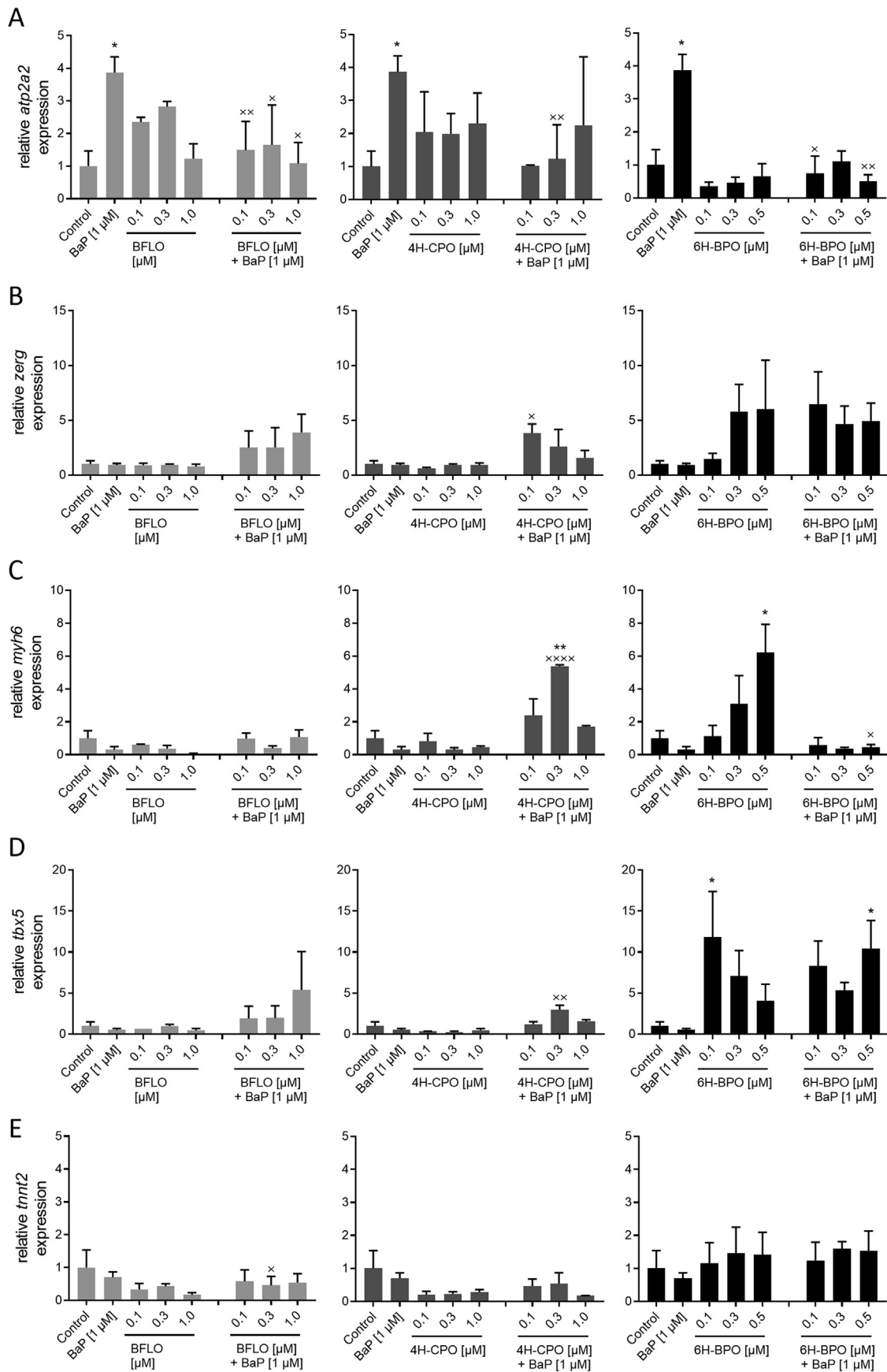
Fig. 2. Relative gene expression of *cyp1a* (A) and *ahr2* (B), and EROD activity (C) in ZFEs exposed to oxy-PAHs alone (0.1–1.0 μM) or in combination with BaP (1 μM) between 24 and 96 hpf. Data are presented as means \pm SE ($n = 2 - 5$). Analysis of statistical differences between each exposure compared to the DMSO control was performed using one-way ANOVA (* $P < 0.05$, ** $P < 0.01$, and *** $P < 0.001$). Student's *t*-test was used for statistical analysis to evaluate whether more or less than additive effects in co-exposures was shown compared to sum of single exposures ($^xP < 0.05$, $^{xx}P < 0.01$, and $^{xxx}P < 0.001$).

compounds bound to the glass petri dish and that 6H-BPO displayed a higher degree of accumulation in the zebrafish embryo compared to BaP. This was also supported by measurements of internal concentrations of 6H-BPO, which increased until a steady-state condition seemed to be reached at 96 hpf (Fig. 6F). Exposure to BaP resulted in a fast uptake in the ZFE up to 27 hpf and decreased thereafter (Fig. 6E). At 96 hpf, an increase in the internal BaP concentration was found, which we could not explain and was therefore treated as an outlier for the toxicokinetic modeling.

In contrast to single compound exposure, the internal concentration of 6H-BPO in the mixture exposure peaked at 27 hpf and decreased thereafter, resulting in a 55-fold lower internal concentration at 96 hpf compared to the exposure of 6H-BPO alone (Fig. 6F). The internal BaP concentration in the mixture exposure also displayed a fast uptake up to 27 hpf that stayed relative stable up to 120 hpf (Fig. 6E). These results suggest a competitive interaction between the two compounds resulting in decreased biotransformation of BaP and increased biotransformation of 6H-BPO.

3.5. Principal component analysis of developmental and cardiovascular toxicity caused by oxy-PAHs and PAHs

To analyze the mixture effects on cardiac developmental toxicity, a principal component analysis (PCA) was conducted on the toxicity and gene expression data presented above. The first and second principal components together explained 56.6% of the variance of the data. The individuals plot identified four clusters (Fig. 7A). The first cluster included the control conditions, BaP, and the three concentrations of 4H-CPO and BFLO, and the lower concentration of 4H-CPO + BaP, which all displayed low or no toxicity to the ZFE. The second cluster consisted of the binary mixtures of 4H-CPO and BFLO with BaP, which, compared to the first group, had a stronger impact on cardiac toxicity and gene expression. The third cluster included 6H-BPO and its binary mixture at 0.1 μM , while the last cluster included the binary mixtures at 0.3 and 0.5 μM 6H-BPO. These last two groups were clearly the most potent in inducing cardiotoxicity and deregulation of gene expression compared to the other groups, and the binary mixtures at higher concentrations



(caption on next page)

Fig. 3. Relative gene expression of genes related with cardiovascular development and function (panels A – E; *atp2a2*, *zerg*, *myh6*, *tbx5*, and *tnnt2*) in ZFEs exposed to oxy-PAHs alone (0.1–1.0 μM) or in combination with BaP (1 μM) between 24 and 96 hpf. Data are presented as means \pm SE ($n = 2$ –5). Analysis of statistical differences between each exposure compared to the DMSO control was performed using one-way ANOVA (* $P < 0.05$, ** $P < 0.01$, and *** $P < 0.001$). Student's *t*-test was used for statistical analysis to evaluate whether more or less than additive effects was observed in co-exposures compared to sum of single exposures ($^{\chi}P < 0.05$, $^{xx}P < 0.01$, and $^{xxx}P < 0.001$).

were additionally potent, as observed by high incidence of string heart formation, and induced expression of *zerg* and *tbx5*. The variables factor map (Fig. 7B) suggested positive correlations between expression of *cyp1a*, *tbx5*, *tnnt2* and pericardial edema (PE) or string heart formation (SH), and negative correlations between expression of *zerg*, *tbx5* and blood flow (BF), which also was confirmed by correlation analyses ($r > 0.5$ and $P < 0.05$, Table S3).

Notably, expression of *cyp1a* was not correlated with EROD activity.

4. Discussion

It is well established that weak or non-carcinogenic PAHs can enhance or reduce the genotoxicity and tumorigenicity of carcinogenic PAHs *in vitro* and *in vivo* (Jarvis et al., 2014). Similarly, PAH mixtures containing AhR agonists and CYP1 inhibitors may cause synergistic and dioxin-like developmental toxicity in fish (Billiard et al., 2008). More recently, the role of polar PACs in the toxicity of environmental PAH pollution has been investigated in more detail (Bandowe and Meusel, 2017; Idowu et al., 2019). Available data show that the polar PAC fraction, including oxy- and nitro-PAHs, of environmental samples may display similar or higher biological activities as the non-polar PAH-containing fraction, including genotoxicity, mutagenicity and developmental effects (Umbuzeiro et al., 2008; Mattsson et al., 2009; Wincent et al., 2015a, McCarrick et al., 2019). We have previously shown that binary oxy-PAH + PAH mixtures induce comparable or greater genotoxic effects than expected compared to the sum effect of single exposure of oxy-PAHs and BaP in ZFE (McCarrick et al., 2019). However, there is a dearth of data on how oxy-PAHs and PAHs present in mixtures might interact in organisms leading to non-additive effects. Based on previous studies employing PAHs (Incardona et al., 2004, 2005, 2011; Van Tiem and Di Giulio, 2011; Brette et al., 2017) or polar PACs (Knecht et al., 2013; Chlebowski et al., 2017; Geier et al., 2018), the cardiovascular system in zebrafish is sensitive to exposure to these compounds and was thus used here to study mixture effects between PAHs and oxy-PAHs. We show that binary mixtures of the oxy-PAHs BFLO or 6H-BPO with BaP, at 1 μM or lower, caused increased developmental and cardiovascular toxicity in ZFEs compared with oxy-PAH or BaP alone. The third oxy-PAH, 4H-CPO was the least potent toxicant, alone and in combination with BaP. The high potency of BFLO and 6H-BPO agrees with previous results from comparative developmental toxicity studies of polar PACs performed in ZFE (Knecht et al., 2013; Geier et al., 2018).

Previous data show that PAHs and PAH mixtures can induce cardiotoxicity in fish in an AhR-dependent or -independent manner, and that this seems to depend on the size and structure of PAHs (Incardona et al., 2004, 2005, 2011; Van Tiem and Di Giulio, 2011; Brette et al., 2017). Our data suggest that mixtures of oxy-PAHs and PAHs also can modulate AhR signaling in ZFE. We show that the expression of *cyp1a* was increased in response to 4H-CPO + BaP and 6H-BPO + BaP and decreased by BFLO + BaP compared with control and BaP alone. BaP, on the other hand, is well-known to be an AhR activator and CYP1 inducer, as was also observed here. Based on our results from *cyp1a* gene expression and EROD activity measurements, 4H-CPO and 6H-BPO seem to be CYP1 inhibitors in ZFE. Although the EROD data is not fully conclusive, and probably due to differences in sensitivity of these methods, the potentiation of *cyp1a* expression by their respective mixtures may be interpreted as a result of decreased metabolism of BaP due to inhibition of CYP1. The lack of *cyp1a* induction by 4H-CPO agrees with a previous study in ZFEs (Geier et al., 2018). The function of 4H-CPO and 6H-BPO as CYP inhibitors is further supported by our previous study using recombinant human CYP1A1 enzyme and HaCaT cells showing that 4H-CPO and 6H-BPO were strong CYP inhibitors (Wincent et al., 2016). The effects on gene expression of *ahr2* displayed a complex pattern. The four tested PACs all significantly reduced *ahr2* expression compared to control when tested as single compounds while two of the mixtures (containing BFLO and 4H-CPO) induced expression levels. The regulation of *ahr2* is not well established although crosstalk with HIF and WNT signaling pathways has been proposed to be important for regulating many of the toxic effects mediated by activation of the AhR (Schneider et al., 2014; Vorrink and Domann, 2014). Indeed, regulation of the crosstalk between the AhR and WNT signaling pathways plays an important role in developmental toxicity in ZFEs (Wincent et al., 2015; Yue et al., 2017). The possible role of WNT signaling in the effects observed needs further investigation.

Previous studies showed that the combination of PAHs that inhibit CYP1 with PAHs that activate AhR might synergistically increase toxicity (Staal et al., 2007; Timme-Laragy AR et al., 2007; Jayasundara et al., 2015). Therefore, the increased toxicity observed here in response to mixture exposure can be due to the interaction between AhR activation and CYP inhibition. The importance of AhR activation was further supported by the almost complete rescue of cardiovascular toxicity in ZFE exposed to 6H-BPO, BaP or their mixture with the protein expression of AhR knocked down by use of morpholinos. Similarly, morpholino knockdown of AhR significantly rescued

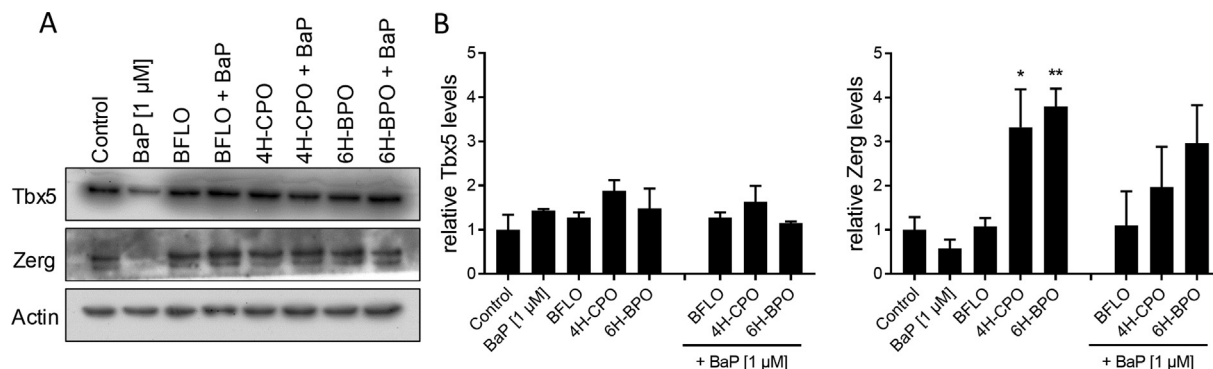


Fig. 4. Protein expression levels of Tbx5 and Zerg (A) in ZFEs exposed to oxy-PAHs alone (0.3 μM) or in combination with BaP (1 μM) between 24 and 96 hpf. Densitometry analysis of normalized expression levels is shown in B. Actin was used as a loading control and DMSO was used as solvent control in all experiments. Data are presented as means \pm SE ($n = 2$ –5) with * $P < 0.05$ as compared to control by one-way ANOVA.

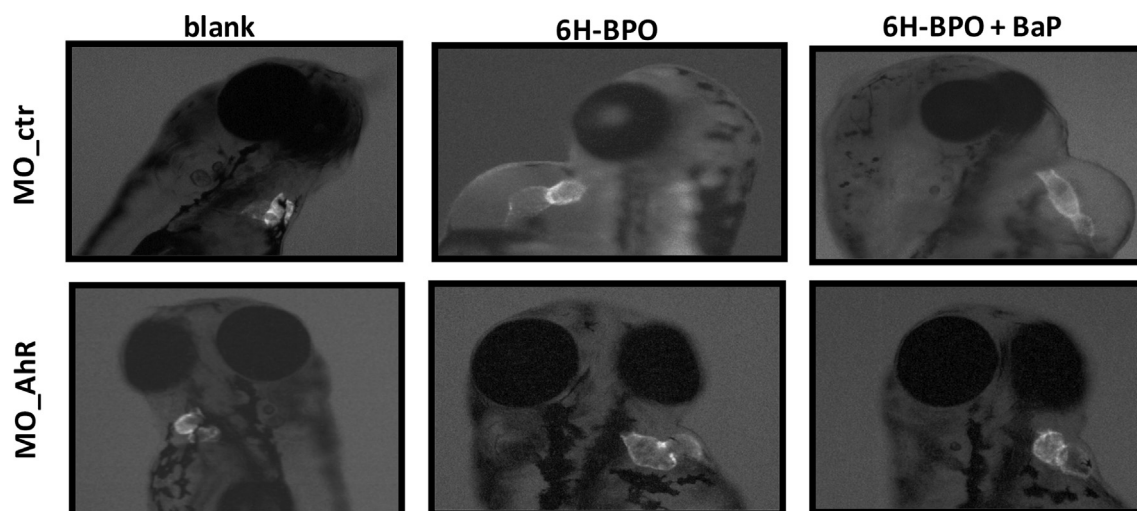


Fig. 5. ZFEs injected with control morpholino (MO_ctr) (top row panels) or with AhR morpholino (MO_AhR) (bottom row panels) exposed to 6H-BPO alone (0.3 μ M) or in combination with BaP (1 μ M) between 24 and 96 hpf. The heart is shown in green given by transgenic zebrafish [Tg (cmlc2:EGFP)]. (For interpretation of the references to colour in this figure legend, the reader is referred to the web version of this article.)

developmental toxicity in ZFE exposed to non-polar and polar fractions of PAC contaminated soil extracts (Wincent et al., 2015a). Knockdown of AhR also rescued developmental effects in ZFE caused by the oxy-PAHs 1,9-benz-10-anthrone and benz[a]anthracene-7,12-dione (Goodale et al., 2015). In addition, CYP1 expression is induced in ZFE by larger oxy-PAHs, but not smaller PAHs such as 4H-CPO (Knecht et al., 2013; Shankar et al., 2019). These data combined suggest that, similar to PAHs, larger oxy-PAHs induce cardiotoxicity in an AhR-dependent manner while smaller compounds do not. We could observe an increase in the heart rate of ZFE injected with MO_AhR exposed to 6H-BPO compared to the MO control. This could be due to AhR influence on genes associated with cardiac function. However, more experiments must be performed to study the mechanism behind this.

To further understand the mechanism of how oxy-PAHs and PAHs might interact to cause cardiotoxicity, we studied expression of genes and proteins involved in heart function (EC coupling), heart development and structure. The results revealed a complex pattern of gene expression changes. In general, the binary mixtures caused reduced expression levels of *atp2a2* and similar or increased expression levels of *zerg* and *tbx5*, compared to single compounds. Principal component analysis revealed that this expression pattern most strongly correlated with effects on blood flow, pericardial edema and, formation of string heart. *Tbx5* plays an important role in heart development as well as a

role in cardiac conduction system function (Moskowitz IP et al., 2004) and transcriptionally activates multiple cardiomyocyte lineage-associated genes including *atp2a2*, *myh6* and *tnnt2*. The gene *atp2a2* is involved in the regulation of heart contraction (Zhu et al., 2008), *myh6* is atrial-specific during the formation of the two chamber zebrafish heart development (England and Loughna, 2013) and *tnnt2* creates the troponin protein complex in cardiac muscle cells (Mikhailov and Torrado, 2016). The association between cardiovascular toxicity induced by environmental pollutants and deregulation of these genes has been studied previously. In mahi (*Coryphaena hippurus*) embryos exposed to crude oil samples from the 2010 Deepwater Horizon disaster, morphological and functional cardiotoxicities was associated with a general down-regulation of cardiac-specific genes, including *tbx5* and *myh6* (Edmunds et al., 2015). In addition, an AHR2-dependent deregulation of gene expression, including *tnnt2*, *myh* and *atp2a1*, was observed in heart tissue from zebrafish embryos exposed to a mixture of BaP and fluoranthene, and prior to onset of cardiac toxicity (Jayasundara et al., 2015). It has furthermore been shown that activation of AhR signaling by TCDD deregulates expression patterns of key cardiogenesis genes, including *tbx5*, in the developing mouse heart, and that this is associated with loss of cardiac function (Carreira et al., 2015). Similarly, TCDD impaired the cardiac differentiation of human embryonic stem cells via the AhR, which involved deregulated expression pattern of

Table 2

Effects on cardiovascular related morphological and functional endpoints in *cmlc2:GFP* ZFEs at 96 hpf injected with MO_ctr or MO_AhR following exposure to 0.3 μ M 6H-BPO alone or in combination with 1 μ M BaP.

		Pericardial edema (%)	String heart (%)	Heartbeat (BPM)	Blood flow (%)
Cmlc2 embryos MO_ctr	Control	0 ^a	0	131 \pm 4	3.2 \pm 0.2
	BaP	2.9 \pm 1.8	0	121 \pm 5	3.0 \pm 0.2
	6H-BPO	50 \pm 10 ^{***}	27 \pm 3.3 ^{***}	109 \pm 4 ^{***}	2.2 \pm 0.2 [*]
	6H-BPO + BaP	60 \pm 5.8 ^{***}	43 \pm 8.8 ^{****}	109 \pm 5 ^{**}	2.6 \pm 0.4
Cmlc2 embryos MO_AhR	Control	0	0	124 \pm 3	3.1 \pm 0.2
	BaP	0	0	124 \pm 5	3.7 \pm 0.3
	6H-BPO	0	0	140 \pm 2 [*] , ^{****}	3.3 \pm 0.2 ^{**}
	6H-BPO + BaP	0	0	135 \pm 5 ^{***}	3.4 \pm 0.3

^a Results are presented as mean \pm standard error, $n = 3 - 10$ replicates for morphological endpoints and $n = 37 - 69$ ZFEs for heartbeat and blood flow.

^{*} $P < 0.05$.

^{***} $P < 0.001$.

^{****} $P < 0.0001$ as compared to control by Kruskal-Wallis (morphological endpoints) or one-way ANOVA (functional endpoints).

^{**} $P > 0.01$.

^{***} $P < 0.001$.

^{****} $P < 0.0001$ as compared to MO_ctr by Student's t -test.

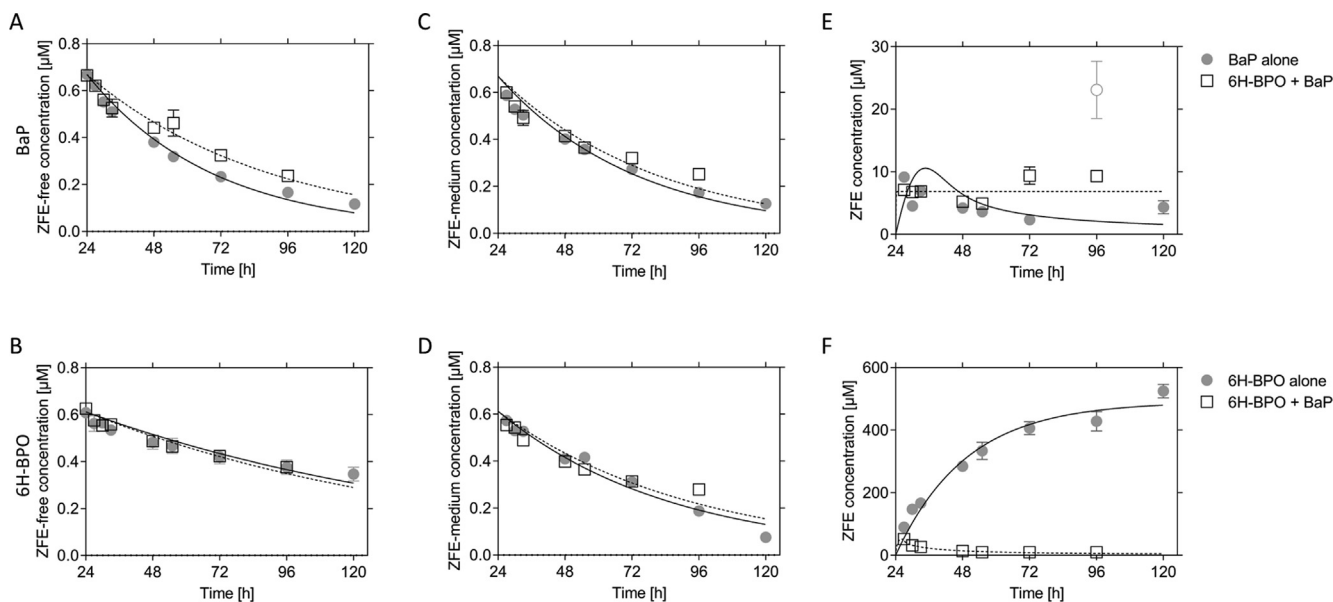


Fig. 6. Time courses of concentrations for 6H-BPO and BaP alone or in combination in ZFE-free medium (A and B), in ZFE-medium (C and D) and in ZFE (E and F). The concentration measurements of the binary mixture were only conducted until 96 hpf due to high lethality at 120 hpf. The lines represent simulated internal concentrations using a one-compartment model. All values are stated as mean ± SE, n = 3–5. See also Table S2.

tbx5 and *tnnt2* among others (Fu et al., 2019). In contrast to our results, upregulation of *tbx5* and *atpa2a2* was associated with an increased heartbeat rate in zebrafish exposed to the flame retardant hexabromocyclododecane (Wu et al., 2013). Zerg protein levels were also increased in embryos exposed to 6H-BPO, 4H-CPO and their mixtures. Notably, cardiotoxicity was associated with reduced gene expression levels of *zerg* (also known as *kcnh2*) in Atlantic haddock embryos exposed to low levels of crude oil (Sorhus et al., 2016). The toxicity was however found to be AhR-independent, which could explain this difference. Altogether, our results indicate complex mechanisms that seem to differ between single oxy-PAHs but also among mixtures.

Activation of the AhR has been shown to induce expression of phase I and phase II biotransformation enzymes, which are responsible for the alteration of toxicokinetic processes of chemicals. To characterize toxicokinetic processes for single PAHs, internal concentrations over time have been measured in rat (Viau et al., 1999), rainbow trout (Kennedy and Law, 1990), Atlantic cod and haddock embryos (Sorensen et al.,

2017) and ZFE (Kuhnert et al., 2013). In accordance with the results presented here, these studies demonstrated that the internal concentrations of PAHs, such as BaP, decrease over time and most likely due to biotransformation as a result of AhR activation and CYP induction. In accordance to our results, Kuehnert et al showed that benz[a]anthracene is biotransformed from 20 hpf old ZFEs (Kuhnert et al., 2013). Wincent et al showed that CYP1 expression levels were induced and enzyme activity enhanced by oxy-PAHs *in vitro* and in ZFE, which indicated a potential capability of biotransformation of these compounds in a comparable manner to PAHs (Wincent et al., 2015a, Wincent et al., 2016). However, there is still limited data on the biotransformation rate of chemicals and identification of biotransformation products in ZFE. To the best of our knowledge, the time course of internal concentrations of oxy-PAHs has not been reported previously.

In agreement with above discussions and implications for mixture effects on biotransformation, the observed time profiles of the internal concentrations for the mixture exposure differed from the single

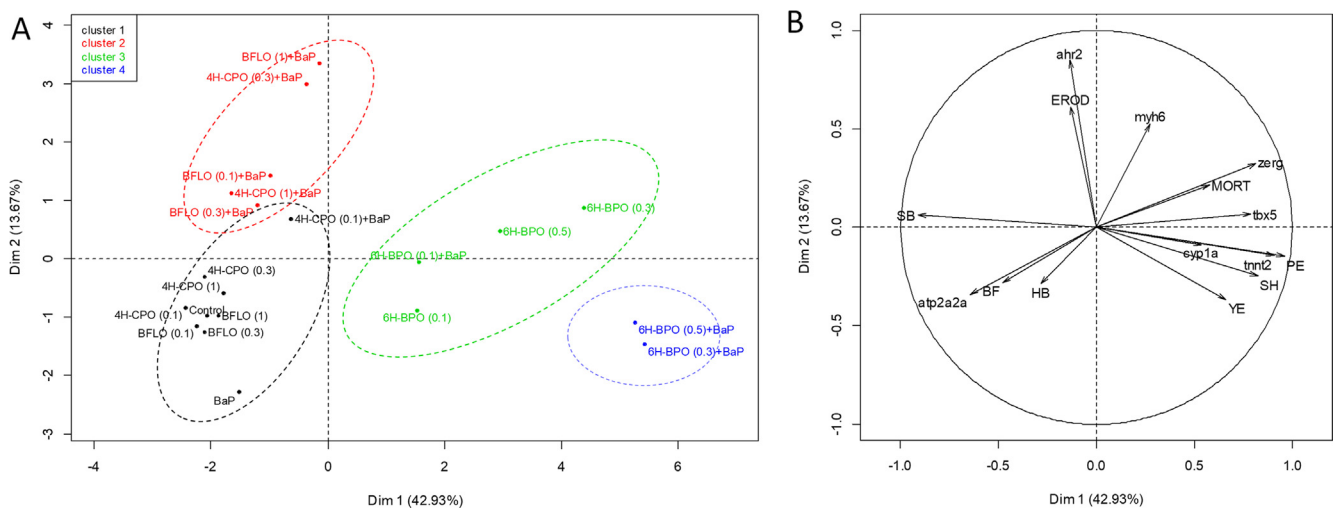


Fig. 7. Principal component analysis of data from ZFE exposed to the three oxy-PAHs, BaP and their mixtures. Panel A shows the individual factor map with four clusters indicated by ellipses and B shows the variables factor map. EROD, MORT, PE, SH, YE, HB, BF and SB stands for EROD activity, mortality, pericardial edema, string heart, yolk-sac edema, heartbeat rate, blood flow, and swim-bladder inflation, respectively. See also Table S3.

exposures. In the mixture exposure, the internal concentration of 6H-BPO significantly decreased over time which was in stark contrast to the apparent accumulation that was observed when exposed as single compound. In contrast, the internal concentration of BaP in the mixture exposure was more stable compared to the single compound exposure which showed a clear decrease over time. These results suggest that 6H-BPO inhibits the metabolism of BaP and is further supported by the observed potentiation of *cyp1a* gene expression which most likely was a result of maintained levels of BaP that can continue to activate the AhR. Together these data further strengthen that 6H-BPO act as a CYP1 inhibitor in ZFE. This observation also suggests that the rapid decrease of 6H-BPO when applied as a mixture was due to an increased biotransformation by other enzymes than CYPs. There is limited transcriptomic data available on oxy-PAHs that could help to discern the induction of possible alternative routes of metabolism. Available data in ZFEs suggest that although certain responses such as redox homeostasis are common, different oxy-PAHs give rise to different gene expression profiles, and with no clear indication of what other types of biotransformation pathways are activated (Goodale et al., 2015; Geier et al., 2018). A possible candidate could be the aldo-keto reductases (AKRs). In mammalian models the AKR1C1 is inducible by planar aromatics and can catalyze oxidation-reduction reactions of PAHs and steroid hormones (Burczynski et al., 1999; Barski et al., 2008). This family of enzymes is not well studied in zebrafish, and only the expression of AKR1A and AKR1B has been confirmed (NCBI Gene database Accessed 2020-04-20b,a).

In conclusion, we show that similar to interactions between PAHs, mixtures of PAHs and oxy-PAHs may cause increased developmental and cardiovascular toxicity in ZFEs through an AhR-dependent mechanism. Our data adds further support to the importance of including oxy-PAHs in risk assessment and monitoring of environmental pollution (Clerge et al., 2019; Idowu et al., 2019). To increase the understanding of the mechanism of action of different oxy-PAHs, and thus a better basis for risk assessment, more data on transcriptomics are clearly needed. In addition, qualitative and quantitative determination of biotransformation products would further help to reveal the biochemical mechanisms of cardiotoxicity as well as other adverse outcomes.

CRedit authorship contribution statement

Virgínia Cunha: Conceptualization, Methodology, Validation, Investigation, Data curation, Writing - original draft, Visualization. **Carolina Vogs:** Conceptualization, Methodology, Validation, Formal analysis, Investigation, Data curation, Writing - original draft, Visualization, Funding acquisition. **Florane Le Bihanic:** Conceptualization, Methodology, Validation, Writing - original draft, Funding acquisition. **Kristian Dreij:** Supervision, Conceptualization, Visualization, Data curation, Formal analysis, Writing - review & editing, Resources, Funding acquisition.

Declaration of Competing Interest

The authors declare that they have no known competing financial interests or personal relationships that could have appeared to influence the work reported in this paper.

Acknowledgement and funding

We thank the zebrafish facility at Karolinska Institutet for excellent service. Authors also acknowledge Dr. Emma Wincent for providing the AhR morpholino and constructive discussions, and the technical support from Ondřej Zapletal and Adegoke Motunrayo. This work was supported by the ÅForsk foundation, Sweden (to K.D. and F.L.B.), the Swedish Research Council Formas (to C.V.), the Swedish Cancer and Allergy foundation (to K.D. and F.L.B.) and a departmental intramural

grant program (to C.V. and K.D.).

Appendix A. Supplementary material

Supplementary data to this article can be found online at <https://doi.org/10.1016/j.envint.2020.105913>.

References

- Bandowe, B.A., Bigalke, M., Boamah, L., Nyarko, E., Saalia, F.K., Wilcke, W., 2014. Polycyclic aromatic compounds (PAHs and oxygenated PAHs) and trace metals in fish species from Ghana (West Africa): bioaccumulation and health risk assessment. *Environ. Int.* 65, 135–146.
- Bandowe, B.A.M., Meusel, H., 2017. Nitroated polycyclic aromatic hydrocarbons (nitro-PAHs) in the environment - A review. *Sci. Total Environ.* 581, 237–257.
- Barski, O.A., Tipparaju, S.M., Bhatnagar, A., 2008. The aldo-keto reductase superfamily and its role in drug metabolism and detoxification. *Drug Metab. Rev.* 40 (4), 553–624.
- Billiard, S.M., Meyer, J.N., Wassenberg, D.M., Hodson, P.V., Di Giulio, R.T., 2008. Nonadditive effects of PAHs on Early Vertebrate Development: mechanisms and implications for risk assessment. *Toxicol. Sci.* 105 (1), 5–23.
- Bradford, M.M., 1976. A rapid and sensitive method for the quantitation of microgram quantities of protein utilizing the principle of protein-dye binding. *Anal. Biochem.* 72, 248–254.
- Brette, F., Machado, B., Cros, C., Incardona, J.P., Scholz, N.L., Block, B.A., 2014. Crude Oil Impairs Cardiac Excitation-Contraction Coupling in Fish. *Science* 343 (6172), 772–776.
- Brette, F., Shiels, H.A., Galli, G.L., Cros, C., Incardona, J.P., Scholz, N.L., Block, B.A., 2017. A Novel Cardiotoxic Mechanism for a Pervasive Global Pollutant. *Sci. Rep.* 7, 41476.
- Brown, D.R., Thompson, J., Chernick, M., Hinton, D.E., Di Giulio, R.T., 2017. Later life swimming performance and persistent heart damage following sublethal PAH mixture exposure in the Atlantic killifish (*Fundulus heteroclitus*). *Environ. Toxicol. Chem.* 36 (12), 3246–3253.
- Burczynski, M.E., Lin, H.K., Penning, T.M., 1999. Isoform-specific induction of a human aldo-keto reductase by polycyclic aromatic hydrocarbons (PAHs), electrophiles, and oxidative stress: implications for the alternative pathway of PAH activation catalyzed by human dihydrodiol dehydrogenase. *Cancer Res.* 59 (3), 607–614.
- Carreira, V.S., Fan, Y., Wang, Q., Zhang, X., Kurita, H., Ko, C.I., Naticchioni, M., Jiang, M., Koch, S., Medvedovic, M., Xia, Y., Rubinstein, J., Puga, A., 2015. Ah receptor signaling controls the expression of cardiac development and homeostasis genes. *Toxicol. Sci.* 147 (2), 425–435.
- Chlebowski, A.C., Garcia, G.R., La Du, J.K., Bisson, W.H., Truong, L., Massey Simonich, S.L., Tanguay, R.L., 2017. Mechanistic investigations into the developmental toxicity of nitroated and heterocyclic PAHs. *Toxicol. Sci.* 157 (1), 246–259.
- Clerge, A., Le Goff, J., Lopez, C., Ledauphin, J., Delepee, R., 2019. Oxy-PAHs: occurrence in the environment and potential genotoxic/mutagenic risk assessment for human health. *Crit. Rev. Toxicol.* 49 (4), 302–328.
- Dasgupta, S., Cao, A., Mauer, B., Yan, B.Z., Uno, S., McElroy, A., 2014. Genotoxicity of oxy-PAHs to Japanese medaka (*Oryzias latipes*) embryos assessed using the comet assay. *Environ. Sci. Pollut. Res.* 21 (24), 13867–13876.
- de Pater, E., Clijsters, L., Marques, S.R., Lin, Y.F., Garavito-Aguilar, Z.V., Yelon, D., Bakkers, J., 2009. Distinct phases of cardiomyocyte differentiation regulate growth of the zebrafish heart. *Development* 136 (10), 1633–1641.
- Edmunds, R.C., Gill, J.A., Baldwin, D.H., Linbo, T.L., French, B.L., Brown, T.L., Esbaugh, A.J., Mager, E.M., Stieglitz, J., Hoenig, R., Benetti, D., Grosell, M., Scholz, N.L., Incardona, J.P., 2015. Corresponding morphological and molecular indicators of crude oil toxicity to the developing hearts of mahi mahi. *Sci. Rep.* 5, 17326.
- England, J., Loughna, S., 2013. Heavy and light roles: myosin in the morphogenesis of the heart. *Cell. Mol. Life Sci.* 70 (7), 1221–1239.
- European Union, 2005. Commission Recommendation of 4 February 2005 on the Further Investigation into the Levels of Polycyclic Aromatic Hydrocarbons in Certain Foods (2005/108/EC). *Official Journal of European Union* L34/43.
- Fu, H., Wang, L., Wang, J., Bennett, B.D., Li, J.L., Zhao, B., Hu, G., 2019. Dioxin and AHR impairs mesoderm gene expression and cardiac differentiation in human embryonic stem cells. *Sci. Total Environ.* 651 (Pt 1), 1038–1046.
- Geier, M.C., Chlebowski, A.C., Truong, L., Massey Simonich, S.L., Anderson, K.A., Tanguay, R.L., 2018. Comparative developmental toxicity of a comprehensive suite of polycyclic aromatic hydrocarbons. *Arch. Toxicol.* 92 (2), 571–586.
- Goodale, B.C., La Du, J., Tilton, S.C., Sullivan, C.M., Bisson, W.H., Waters, K.M., Tanguay, R.L., 2015. Ligand-Specific Transcriptional Mechanisms Underlie Aryl Hydrocarbon Receptor-Mediated Developmental Toxicity of Oxygenated PAHs. *Toxicol. Sci.* 147 (2), 397–411.
- Holme, J.A., Brinchmann, B.C., Refsnes, M., Lag, M., Ovrevik, J., 2019. Potential role of polycyclic aromatic hydrocarbons as mediators of cardiovascular effects from combustion particles. *Environ Health* 18 (1), 74.
- IARC 2010. Some Non-heterocyclic Polycyclic Aromatic Hydrocarbons and Some Related Exposures. *IARC Monographs on the Evaluation of Carcinogenic Risks to Humans* 92.
- Idowu, O., Semple, K.T., Ramadass, K., O'Connor, W., Hansbro, P., Thavamani, P., 2019. Beyond the obvious: Environmental health implications of polar polycyclic aromatic hydrocarbons. *Environ. Int.* 123, 543–557.
- Incardona, J.P., Carls, M.G., Holland, L., Linbo, T.L., Baldwin, D.H., Myers, M.S., Peck, K.A., Tagal, M., Rice, S.D., Scholz, N.L., 2015. Very low embryonic crude oil

- exposures cause lasting cardiac defects in salmon and herring. *Sci. Rep.* 5.
- Incardona, J.P., Carls, M.G., Teraoka, H., Sloan, C.A., Collier, T.K., Scholz, N.L., 2005. Aryl hydrocarbon receptor-independent toxicity of weathered crude oil during fish development. *Environ. Health Perspect.* 113 (12), 1755–1762.
- Incardona, J.P., Collier, T.K., Scholz, N.L., 2004. Defects in cardiac function precede morphological abnormalities in fish embryos exposed to polycyclic aromatic hydrocarbons. *Toxicol. Appl. Pharmacol.* 196 (2), 191–205.
- Incardona, J.P., Gardner, L.D., Linbo, T.L., Brown, T.L., Esbaugh, A.J., Mager, E.M., Stieglitz, J.D., French, B.L., Labenia, J.S., Laetz, C.A., Tagal, M., Sloan, C.A., Elizur, A., Benetti, D.D., Grosell, M., Block, B.A., Scholz, N.L., 2014. Deepwater Horizon crude oil impacts the developing hearts of large predatory pelagic fish. *Proc. Natl. Acad. Sci. USA* 111 (15), E1510–E1518.
- Incardona, J.P., Linbo, T.L., Scholz, N.L., 2011. Cardiac toxicity of 5-ring polycyclic aromatic hydrocarbons is differentially dependent on the aryl hydrocarbon receptor 2 isoform during zebrafish development. *Toxicol. Appl. Pharmacol.* 257 (2), 242–249.
- Jarvis, I.W., Dreij, K., Mattsson, Å., Jernström, B., Stenius, U., 2014. Interactions between PAHs in complex mixtures and implications for cancer risk assessment. *Toxicology* 321, 27–39.
- Jayasundara, N., Van Tiem Garner, L., Meyer, J.N., Erwin, K.N., Di Giulio, R.T., 2015. AHR2-Mediated transcriptomic responses underlying the synergistic cardiac developmental toxicity of PAHs. *Toxicol. Sci.* 143 (2), 469–481.
- Kennedy, C.J., Law, F.C.P., 1990. Toxicokinetics of selected polycyclic aromatic hydrocarbons in rainbow-trout following different routes of exposure. *Environ. Toxicol. Chem.* 9 (2), 133–139.
- Knecht, A.L., Goodale, B.C., Truong, L., Simonich, M.T., Swanson, A.J., Matzke, M.M., Anderson, K.A., Waters, K.M., Tanguay, R.L., 2013. Comparative developmental toxicity of environmentally relevant oxygenated PAHs. *Toxicol. Appl. Pharmacol.* 271 (2), 266–275.
- Korashy, H.M., El-Kadi, A.O.S., 2006. The role of aryl hydrocarbon receptor in the pathogenesis of cardiovascular diseases. *Drug Metab. Rev.* 38 (3), 411–450.
- Kuhnert, A., Vogts, C., Altenburger, R., Kuster, E., 2013. The internal concentration of organic substances in fish embryos—a toxicokinetic approach. *Environ. Toxicol. Chem.* 32 (8), 1819–1827.
- Layshock, J.A., Wilson, G., Anderson, K.A., 2010. Ketone and quinone-substituted polycyclic aromatic hydrocarbons in mussel tissue, sediment, urban dust, and diesel particulate matrices. *Environ. Toxicol. Chem.* 29 (11), 2450–2460.
- Le Bihanic, F., Sommar, V., Perrine de, L., Pichon, A., Grasset, J., Berrada, S., Budzinski, H., Cousin, X., Morin, B., Cachot, J., 2015. Environmental concentrations of benz[a]anthracene induce developmental defects and DNA damage and impair photomotor response in Japanese medaka larvae. *Ecotoxicol. Environ. Saf.* 113, 321–328.
- Le, S., Josse, J., Husson, F., 2008. FactoMineR: An R package for multivariate analysis. *J. Stat. Softw.* 25 (1), 1–18.
- Lundstedt, S., White, P.A., Lemieux, C.L., Lynes, K.D., Lambert, I.B., Oberg, L., Haglund, P., Tysklind, M., 2007. Sources, fate, and toxic hazards of oxygenated polycyclic aromatic hydrocarbons (PAHs) at PAH-contaminated sites. *Ambio* 36 (6), 475–485.
- MacRae, C.A., Peterson, R.T., 2015. Zebrafish as tools for drug discovery. *Nat. Rev. Drug Discovery* 14 (10), 721–731.
- Mattsson, Å., Lundstedt, S., Stenius, U., 2009. Exposure of HepG2 cells to low levels of PAH-containing extracts from contaminated soils results in unpredictable genotoxic stress responses. *Environ. Mol. Mutagen.* 50 (4), 337–348.
- McCarrick, S., Cunha, V., Zapletal, O., Vondracek, J., Dreij, K., 2019. In vitro and in vivo genotoxicity of oxygenated polycyclic aromatic hydrocarbons. *Environ. Pollut.* 246, 678–687.
- Mikhailov, A.T., Torrado, M., 2016. Myocardial transcription factors in diastolic dysfunction: clues for model systems and disease. *Heart Fail. Rev.* 21 (6), 783–794.
- Miura, G.I., Deborah, Y., 2011. A guide to analysis of cardiac phenotypes in the zebrafish embryo. *Methods Cell Biol.* 101, 161–180.
- Moskowitz, I.P., Pizard, A., Patel, V.V., Bruneau, B.G., Kim, J.B., Kupersmidt, S., Roden, D., Berul, C.I., Seidman, C.E., Seidman, Jonathan G., 2004. The T-Box transcription factor Tbx5 is required for the patterning and maturation of the murine cardiac conduction system. *Development* 131(16), 4107–4116.
- NCBI Gene database Accessed 2020-04-20a. <https://www.ncbi.nlm.nih.gov/gene/415138>, akr1b1.1 aldo-keto reductase family 1, member B1 (aldose reductase), tandem duplicate 1 [Danio rerio (zebrafish)].
- NCBI Gene database Accessed 2020-04-20b. <https://www.ncbi.nlm.nih.gov/gene/445326>, akr1a1a aldo-keto reductase family 1, member A1a (aldehyde reductase) [Danio rerio (zebrafish)].
- Perrichon, P., Le Bihanic, F., Bustamante, P., Le Menach, K., Budzinski, H., Cachot, J., Cousin, X., 2014. Influence of sediment composition on PAH toxicity using zebrafish (Danio rerio) and Japanese medaka (*Oryzias latipes*) embryo-larval assays. *Environ. Sci. Pollut. Res.* 21 (24), 13703–13719.
- Prasch, A.L., Teraoka, H., Carney, S.A., Dong, W., Hiraga, T., Stegeman, J.J., Heideman, W., Peterson, R.E., 2003. Aryl hydrocarbon receptor 2 mediates 2,3,7,8-tetrachlorodibenzo-p-dioxin developmental toxicity in zebrafish. *Toxicol. Sci.* 76 (1), 138–150.
- Sarmah, S., Marrs, J., 2016. Zebrafish as a vertebrate model system to evaluate effects of environmental toxicants on cardiac development and function. *Int. J. Mol. Sci.* 17 (12), 2123.
- Schneider, A.J., Branam, A.M., Peterson, R.E., 2014. Intersection of AHR and Wnt signaling in development, health, and disease. *Int. J. Mol. Sci.* 15 (10), 17852–17885.
- Shankar, P., Geier, M.C., Truong, L., McClure, R.S., Pande, P., Waters, K.M., Tanguay, R.L., 2019. Coupling genome-wide transcriptomics and developmental toxicity profiles in zebrafish to characterize polycyclic aromatic hydrocarbon (PAH) hazard. *Int. J. Mol. Sci.* 20 (10).
- Sorensen, L., Sorhus, E., Nordtug, T., Incardona, J.P., Linbo, T.L., Giovanetti, L., Karlsen, O., Meier, S., 2017. Oil droplet fouling and differential toxicokinetics of polycyclic aromatic hydrocarbons in embryos of Atlantic haddock and cod. *PLoS ONE* 12 (7), e0180048.
- Sorhus, E., Incardona, J.P., Karlsen, O., Linbo, T., Sorensen, L., Nordtug, T., van der Meer, T., Thorsen, A., Thorbjornsen, M., Jentoft, S., Edvardsen, R.B., Meier, S., 2016. Crude oil exposures reveal roles for intracellular calcium cycling in haddock craniofacial and cardiac development. *Sci. Rep.* 6.
- Staal, Y.C.M., Hebels, D.G.A.J., van Herwijnen, M.H.M., Gottschalk, R.W.H., van Schooten, F.J., van Delft, J.H.M., 2007. Binary PAH mixtures cause additive or antagonistic effects on gene expression but synergistic effects on DNA adduct formation. *Carcinogenesis* 28 (12), 2632–2640.
- Timme-Laragy, A.R., Cockman, C.J., Matson, C.W., Di Giulio, Richard T., 2007. Synergistic induction of AHR regulated genes in developmental toxicity from co-exposure to two model PAHs in zebrafish. *Aquat. Toxicol.* 85(4), 241–250.
- U.S. EPA, 2010. Development of a Relative Potency Factor (RPF) Approach for Polycyclic Aromatic Hydrocarbon (PAH) Mixtures: In: Support of Summary Information on the Integrated Risk Information System (IRIS). EPA/635/R-08/012A. U. S. EPA. Washington D.C.
- Umbuzeiro, G.A., Franco, A., Martins, M.H., Kummrow, F., Carvalho, L., Schmeider, H.H., Leykauf, J., Stiborova, M., Claxton, L.D., 2008. Mutagenicity and DNA adduct formation of PAH, nitro-PAH, and oxy-PAH fractions of atmospheric particulate matter from Sao Paulo, Brazil. *Mutat. Res.* 652 (1), 72–80.
- Van Tiem, L.A., Di Giulio, R.T., 2011. AHR2 knockdown prevents PAH-mediated cardiac toxicity and XRE- and ARE-associated gene induction in zebrafish (Danio rerio). *Toxicol. Appl. Pharmacol.* 254 (3), 280–287.
- Viau, C., Bouchard, M., Carrier, G., Brunet, R., Krishnan, K., 1999. The toxicokinetics of pyrene and its metabolites in rats. *Toxicol. Lett.* 108 (2–3), 201–207.
- Vogts, C., Johanson, G., Näslund, M., Wulff, S., Sjödin, M., Hellstrandh, M., Lindberg, J., Wincent, E., 2019. Toxicokinetics of perfluorinated alkyl acids influences their toxic potency in the zebrafish embryo (Danio rerio). *Environ. Sci. Technol.* 53 (7), 3898–3907.
- Vorriuk, S.U., Domann, F.E., 2014. Regulatory crosstalk and interference between the xenobiotic and hypoxia sensing pathways at the AhR-ARNT-HIF1 alpha signaling node. *Chem. Biol. Interact.* 218, 82–88.
- Wincent, E., Stegeman, J.J., Jönsson, M.E., 2015. Combination effects of AHR agonists and Wnt/beta-catenin modulators in zebrafish embryos: Implications for physiological and toxicological AHR functions. *Toxicol. Appl. Pharmacol.* 284 (2), 163–179.
- Wincent, E., Jönsson, M.E., Bottai, M., Lundstedt, S., Dreij, K., 2015a. Aryl hydrocarbon receptor activation and developmental toxicity in zebrafish in response to soil extracts containing unsubstituted and oxygenated PAHs. *Environ. Sci. Technol.* 49 (6), 3869–3877.
- Wincent, E., Le Bihanic, F., Dreij, K., 2016. Induction and inhibition of human cytochrome P4501 by oxygenated polycyclic aromatic hydrocarbons. *Toxicol. Res.* (Camb) 5 (3), 788–799.
- Wu, M.F., Zuo, Z.H., Li, B.W., Huang, L.X., Chen, M., Wang, C.G., 2013. Effects of low-level hexabromocyclododecane (HBCD) exposure on cardiac development in zebrafish embryos. *Ecotoxicology* 22 (8), 1200–1207.
- Yue, C., Ji, C., Zhang, H., Zhang, L.W., Tong, J., Jiang, Y., Chen, T., 2017. Protective effects of folic acid on PM2.5-induced cardiac developmental toxicity in zebrafish embryos by targeting AhR and Wnt/beta-catenin signal pathways. *Environ. Toxicol.* 32 (10), 2316–2322.
- Zhu, Y., Gramolini, A.O., Walsh, M.A., Zhou, Y.Q., Slorach, C., Friedberg, M.K., Takeuchi, J.K., Sun, H., Henkelman, R.M., Backx, P.H., Redington, A.N., MacLennan, D.H., Bruneau, B.G., 2008. Tbx5-dependent pathway regulating diastolic function in congenital heart disease. *PNAS* 105 (14), 5519–5524.